may cause the two heme edges to be further away in cytochrome *c* than in *c*-551, even when the orientation is correct for electron transfer. The greater the distance between the two hemes, the slower the rate of electron transfer, consistent with the larger self-exchange rate constant in *c*-551. A similar effect has been invoked to explain the observation that cytochrome b_5 reconstituted with protohemin dimethyl ester has a large self-exchange rate constant than the native protein (7.6×10^2 and 11 M^{-1} s^{-1}, respectively).[101] The esterified hemin has neutral, rather than negatively charged, propionate side chains.

The discussion above has assumed that electron transfer takes place only through the exposed heme edge. However, electron transfer has been shown to occur through the protein in some instances. For example, electron transfer between cytochrome *c* peroxidase and cytochrome *c* occurs with a second-order rate constant of $\sim 10^8$ M^{-1} s^{-1}. A computer-graphics-generated model for the electron-transfer complex shows that the two hemes are parallel, with an edge separation of ~ 17 Å. This is the closest possible approach due to the location of the peroxidase heme in the interior of the protein. Thus, in this case an electron is transferred rapidly over a long distance.[13]

Electron transfer through the protein has also been demonstrated in a number of studies on derivatized heme proteins. Gray[102] and Isied[4,103] and their co-workers have investigated ruthenium derivatives of cytochrome *c* and shown that intramolecular electron transfer takes place over ~ 12 Å (k = 30–50 s^{-1}, $\Delta G^\circ \simeq -4.5$ kcal mol^{-1}). Hoffman and co-workers have replaced one of the hemes in hemoglobin with a zinc porphyrin and shown that electron transfer occurs between the Zn and Fe centers (photoexcitation of ZnP, $k \approx 60$ s^{-1}, $\Delta E' = 0.6$ V, heme edge-to-edge distance ~ 20 Å).[104] Simolo et al. have shown intramolecular electron transfer within the $\alpha_2^{Zn}\beta_2^{Fe^{III}CN}{}_{Hb}$/ferricytochrome b_5 complex ($k \approx 8 \times 10^3$ s^{-1}, heme edge-to-edge distance ~ 7 Å) and Zn(cytochrome *c*)/cytochrome b_5 complex ($k \approx 4 \times 10^5$ s^{-1}, heme edge-to-edge distance ~ 8 Å).[105] Direct comparison with the self-exchange studies is difficult, because $\Delta G^\circ \neq 0$ in these systems. However, the observation that electron transfer can occur through the protein may in part explain the observation that electron exchange in model hemes is only approximately 10-fold faster than that in the small cytochromes.

Conclusions

Bis(imidazole)iron prophyrins have self-exchange rate constants that do not depend on variations in steric bulk on either the heme periphery or axial imidazole. The rate constants are smaller for complexes with imidazoles bearing an N–H, rather than an *N*-alkyl, substituent. Hydrogen bonding or complete deprotonation of the axial imidazole nitrogen atom may play a role in controlling electron transfer in heme proteins. The rate constants for model hemes (10^7–10^8 M^{-1} s^{-1}) are only approximately a factor of 10 larger than those found in the small cytochromes. This observation, together with data on the proteins themselves, argues that heme exposure is not the major determinant in controlling the rate constant for electron self-exchange in cytochromes.

Acknowledgment. We thank the National Institutes of Health (Grants AM 30479 and BRSG S07 RR07054) for support of this work.

Registry No. Fe(TPP)(1-MeIm)$_2$, 54032-54-1; Fe(3-MeTPP)(1-MeIm)$_2$, 74964-83-3; Fe(4-MeTPP)(1-MeIm)$_2$, 85538-93-8; Fe(4-OMeTPP)(1-MeIm)$_2$, 85529-45-9; Fe(2,4,6-Me$_3$TPP)(1-MeIm)$_2$, 93110-26-0; Fe(TPP)(1-*n*-BuIm)$_2$, 71768-83-7; Fe(TPP)(1-*t*-Bu-5-MeIm)$_2$, 96666-14-7; Fe(3-MeTPP)(5-MeIm)$_2$, 96666-15-8; Fe(3-MeTPP)(5-*t*-BuIm)$_2$, 96688-71-0; Fe(3-MeTPP)(Im)$_2$, 96666-16-9.

(101) Reid, L. S.; Mauk, M. R.; Mauk, A. G. *J. Am. Chem. Soc.* **1984**, *106*, 2182–2185.
(102) Nocera, D. G.; Winkler, J. R.; Yocom, K. M.; Bordignon, E.; Gray, H. B. *J. Am. Chem. Soc.* **1984**, *106*, 5145–5150.
(103) Isied, S. S.; Kuehn, C.; Worosila, G. *J. Am. Chem. Soc.* **1984**, *106*, 1722–1726.
(104) Peterson-Kennedy, S. E.; McGourty, J. L.; Hoffman, B. M. *J. Am. Chem. Soc.* **1984**, *106*, 5010–5012.
(105) Simolo, K. P.; McLendon, G. L.; Mauk, M. R.; Mauk, A. G. *J. Am. Chem. Soc.* **1984**, *106*, 5012–5013.

Contribution from the Chemical Research Institute of Non-aqueous Solutions, Tohoku University, Katahira, Sendai 980, Japan, and Pharmaceutical Institute, Tohoku University, Aobayama, Sendai 980, Japan

Characterization of (Tetrabenzoporphinato)iron

NAGAO KOBAYASHI,*† MASAMI KOSHIYAMA,‡ and TETSUO OSA*‡

Received November 1, 1984

(Tetrabenzoporphinato)iron chloride (ClFeTBP) was characterized by cyclic voltammetry, by EPR, optical absorption, and magnetic circular dichroism (MCD) spectroscopy, and by conductance measurements. ClFeTBP is a pentacoordinated iron(III) high-spin-state complex. However, the extent of dissociation of the Fe–Cl bond is larger than that in (*meso*-tetraphenylporphinato)iron(III) chloride (ClFe^{III}TPP). As with other iron(III) porphyrins, electrochemical or chemical reduction of ClFe^{III}TBP seems to produce stepwise iron(II) and iron(I) complexes and chemical oxidation gives the Fe^{III}TBP π cation radical. Unlike most porphyrins, optically pure and stable mono- and bis(imidazole) complexes are obtained; they are both iron(III) low-spin-state complexes. EPR data suggest ClFeTBP in pyridine exists as a mixture of iron(III) high- and intermediate-spin complexes. The results are examined in comparison with those for iron porphyrins and hemes previously studied and are of interest since tetrabenzoporphyrins are structurally intermediary between general porphyrins and phthalocyanines.

Introduction

Iron porphyrins (FePor's) and phthalocyanines (FePc's) have been the subjects of extensive studies. However, there is little information[1-3] on FeTBP, a structural intermediate of FePor's and FePc's, because of the difficulty in its synthesis.[4] Even the oxidation and spin states of the central iron have not been clarified. Since FePor's generally favor the iron(III) state and FePc's the iron(II) state under air,[5] such studies of FeTBP are of fundamental importance. Other thermodynamic and spectroscopic properties have also been expected to be between those of normal FePor's and FePc's.[6] As will be described below, Fe^{III}TBP exhibited, in many respects, properties intermediate between those of normal

† Chemical Research Institute of Non-aqueous Solutions.
‡ Pharmaceutical Institute.

(1) Synthesis procedures and preliminary results have been published: Kobayashi, N.; Koshiyama, M.; Osa, T. *Chem. Lett.* **1983**, 163–166.
(2) (a) Volger, A.; Retwisch, B.; Kunkerly, H.; Huttermann, J.: (a) *Angew. Chem., Int. Ed. Engl.* **1978**, *17*, 952–953; (b) *Inorg. Chim. Acta* **1980**, *46*, 101–105.
(3) (a) Sams, J. R.; Tsin, T. B. *Chem. Phys. Lett.* **1974**, *25*, 599–601. (b) Koehorst, R. B. M.; Kleibeuker, J. F.; Schaafsma, T. J.; de Bie, D. A.; Geurtsen, B.; Henrie, R. N.; van der Plas, H. C. *J. Chem. Soc., Perkin Trans. 2* **1981**, 1005–1009.
(4) Linstead, R. P.; Noble, E. G. *J. Chem. Soc.* **1937**, 933–936.
(5) Lever, A. B. P. *Adv. Inorg. Chem. Radiochem.* **1965**, *7*, 27–114.
(6) Gouterman, M. In "The Porphyrins"; Dolphin, D., Ed.; Academic Press: New York, London, 1979; Vol. 3, pp 1–165.

0020-1669/85/1324-2502$01.50/0

Table I. Principal g Values and Energy Differences between t_{2g} Orbitals of Imidazole Adducts of Porphyrin Complexes

complexes	principal g values			coeff of basis function			tetragonal splitting (μ) in λ^l	rhombic splitting (R) in λ^l	ref[h]
	g_x	g_y	g_z	A_1	B_1	C_1			
ClImFeTBP	1.63	2.34	2.71	0.965	−0.222	−0.136	1.71	1.68	this work
$Cl(Im)_2FeTBP$	1.62	2.32	2.76	0.966	−0.224	−0.133	1.77	1.68	this work
$Cl(Im)_2FePP$[a]	1.56	2.28	2.90	0.963	−0.249	−0.134	3.33	2.00	*e*
$Cl(Im)_2FePPD$[b]	1.68	2.28	2.80	0.974	−0.215	−0.115	3.82	2.37	*e*
$Mb(Fe^{3+})Im$[c]	1.53	2.26	2.91	0.958	−0.256	−0.135	3.32	1.93	*f*
$Cl(Im)_2FeTPP$[d]	1.5	2.3	2.9	0.956	−0.257	−0.147	2.95	1.93	*g*

[a] PP = protohemin. [b] PPD = protohemin dimethyl ester. [c] Mb = myoglobin. [d] TPP = *meso*-tetraphenylporphine. [e] Reference 15. [f] Hori, H. *Biochim. Biophys. Acta* **1971**, *251*, 227. [g] LaMar, N.; Walker, F. A. *J. Am. Chem. Soc.* **1973**, *95*, 1782. [h] Data in the present work were collected at 7.1–7.6 K, while those in ref *e*–*g* were collected at 77 K. [l] $\lambda \approx 400$ cm^{-1}.

Fe^{III} porphyrins and the mononuclear Fe^{III} Pc's recently reported.[7]

Experimental Section

(i) Materials. A method for ClFeTBP synthesis and purification has been developed and reported.[1] $ClFe^{III}TPP$ and $BrFe^{III}TPP$ were prepared from $(FeTPP)_2O$ according to the literature.[8] The solvents (DMF, pyridine, Me_2SO, $CHCl_3$, CH_2Cl_2, benzene, chlorobenzene, CH_3OH, THF, and acetone) and supporting electrolytes (tetraethylammonium perchlorate (Et_4NClO_4), LiCl, LiBr, and $LiClO_4$) were purified by standard techniques.[9-11] Phenoxathiin hexachloroantimonate, an oxidation reagent, was prepared by the method of Reed et al.[12]

A small rectangular optically transparent thin-layer electrode (OTTLE) cell containing a platinum minigrid working electrode was constructed according to the literature.[13] The OTTLE could be placed in the cell holders of the absorption and MCD apparatus.

(ii) Measurement. Absorption spectra were measured with a Jasco Uvidec-1 spectrophotometer. MCD spectra were recorded with a Jasco J-400X spectrodichrometer equipped with a data processor and an electromagnet that produced magnetic fields up to 1.17 T, with parallel and antiparallel fields. An S-1 type photomultiplier (Hamamatsu Television) was used as the detector for the wavelength region from 700 to 1000 nm. The field magnitude is expressed in terms of molar ellipticity per tesla (1 T = 10 000 G), $[\theta]_M$/deg mol^{-1} dm^3 cm^{-1} T^{-1}. The absorption and MCD cells had path lengths of 1 and 10 mm and were used at ambient temperature; the path length of the OTTLE was 1 mm. Experiments using the OTTLE were conducted under nitrogen atmosphere, and the potentials were supplied by a potentiostat built according to the literature.[14] For low-temperature MCD spectral measurements, a cell with a path length of 2 mm equipped with a Cu(Au–Co) thermocouple was placed in a quartz Dewar. The temperature was regulated by a stream of cold nitrogen gas from a container of liquid nitrogen. EPR spectra were recorded on a Varian E0112 X-band spectrometer equipped with tapered ring-shim tips and with an Oxford EPR 9 cryostat. The microwave frequencies were monitored by a Takedariken TR-5501 frequency counter with a TR-5023 frequency converter. A model CM-30ET conductivity meter (TOA Electronics Ltd.) was used to measure solution conductances. Measurements were taken in a Model GD-201PL cell (cell constant 1.015 cm^{-1}), which was immersed in a constant-temperature bath at 25 ± 0.1 °C. All values are reported as molar conductances.

Cyclic voltammetric sweeps were generated by an NF circuit design block FG-100AD function generator in conjunction with the above mentioned potentiostat. A three-electrode configuration was employed, with a glassy-carbon (Tokai GC-20) working electrode, a platinum-wire auxiliary electrode, and a SCE reference that was connected to the solution either by a double bridge containing saturated KCl solution or by a porous Vycor rod impregnated with solvent and supporting electrolyte.

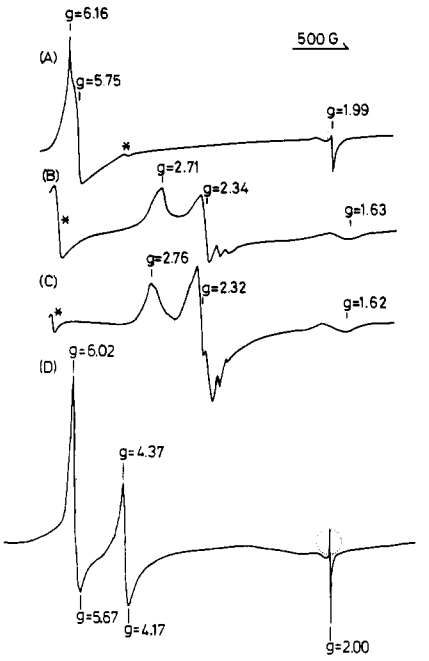

Figure 1. EPR spectra of (A) $ClFe^{III}TBP$ in $CHCl_3$–MeOH (1:1 v/v), (B) $ClImFe^{III}TBP$ in $CHCl_3$–MeOH (1:1 v/v) ($[ClFe^{III}TBP]/M = 2.5 \times 10^{-5}$, $[Im]/M = 5 \times 10^{-2}$), (C) $Cl(Im)_2Fe^{III}TBP$ in DMF ($[ClFe^{III}TBP]/M = 2 \times 10^{-5}$, $[Im]/M = 5$), and (D) $ClFe^{III}TBP$ in pyridine at 6.7, 7.1, 7.6, and 7.0 K, respectively, showing g values. With the decrease in temperature, the intensity of the signal surrounded by the dotted circle reduced significantly. Asterisks indicate noise from quartz.

Results and Discussion

(i) Electron Paramagnetic Resonance. EPR spectra were recorded for only four complexes. The spectrum of $ClFe^{III}TBP$ is shown in Figure 1, curve A. A signal of g value 1.99 was observed at temperatures lower than ca. 30 K, but that of $g = 6$ appeared at ca. 15 K and grew markedly in the <10 K region, indicating that $ClFe^{III}TBP$ is an Fe(III) high-spin complex.[15]

In the presence of an appropriate amount of imidazole (Im) in $CHCl_3$ or $CHCl_3$–MeOH (1:1 v/v), a mono(imidazole) adduct of $ClFe^{III}TBP$, tentatively designated as $ClImFe^{III}TBP$, was formed. Similarly, a bis(imidazole) complex, $Cl(Im)_2Fe^{III}TBP$, was formed in DMF (for details, see part v). These complexes showed spectra characteristic of an Fe(III) low-spin-state complex[15,16] at temperatures lower than 20 K (curves B and C). Because of the presence of three signals, the symmetry around iron(III) was found to be lowered to a rhombic symmetry. In addition, the g_z values for these complexes were slightly smaller than those of bis(imidazole) complexes of normal Fe^{III} porphyrins.[17,18] Using the complete sets of the g values for low-spin

(7) (a) Kobayashi, N.; Koshiyama, M.; Funayama, K.; Osa, T.; Shirai, H.; Hanabusa, K. *J. Chem. Soc., Chem. Commun.* **1983**, 913–914. (b) Kobayashi, N.; Koshiyama, M.; Ishikawa, Y.; Osa, T.; Shirai, H.; Hojo, N. *Chem. Lett.* **1984**, 1633–1636. (c) Kobayashi, N.; Koshiyama, M.; Ishikawa, Y.; Osa, T.; Shirai, H.; Hojo, N., submitted for publication in *J. Am. Chem. Soc.*
(8) Bottomley, L. A.; Kadish, K. M. *Inorg. Chem.* **1981**, *20*, 1348–1357.
(9) Mann, C. K. *J. Electroanal. Chem. Interfacial Electrochem.* **1969**, *3*, 57.
(10) Meites, L. "Polarographic Techniques", 2nd ed.; Interscience: New York, 1965.
(11) Riddick, J. A.; Bunger, W. B. In "Techniques of Chemistry"; Weisberger, A., Ed.; Wiley-Interscience: New York, 1970; Vol. 2.
(12) Gans, P.; Marchon, J. C.; Reed, C. A. *Nouv. J. Chim.* **1981**, *5*, 203–204.
(13) (a) DeAngellis, T. P.; Heineman, W. R. *J. Chem. Educ.* **1976**, *53*, 594–597. (b) Anderson, C. W.; Halsal, H. B.; Heineman, W. R. *Anal. Biochem.* **1979**, *93*, 366–371.
(14) Kuwana, T.; Storojek, J. W. *Discuss. Faraday Soc.* **1968**, *No. 45*, 134–144.
(15) Palmer, G. In "The Porphyrins"; Dolphin, D., Ed.; Academic Press: New York, London, 1979; Vol. 4, pp 313–353.
(16) Salmeen, I.; Palmer, G. *J. Chem. Phys.* **1968**, *48*, 2049–2052.
(17) Yoshimura, T.; Ozaki, T.; Shintani, Y. *J. Inorg. Nucl. Chem.* **1977**, *185*, 39–44.
(18) Migita, C. T.; Iwaizumi, M. *J. Am. Chem. Soc.* **1981**, *103*, 4378–4381.

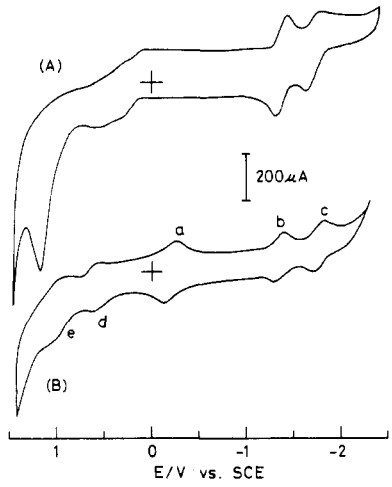

Figure 2. Cyclic voltammograms of (A) tetrabenzoporphine (H_2TBP) and (B) $ClFe^{III}TBP$ in N_2-saturated DMF containing 0.1 M TEAP (scan rate 0.126 V s^{-1}, area of electrode (glassy carbon) 0.77 cm^2, $[H_2TBP]/M = 1.5 \times 10^{-3}$, and $[ClFe^{III}TBP]/M = 8.0 \times 10^{-4}$).

Table II. Voltammetric Data for ClFeTBP[b]

		$E_{1/2}$/V vs. SCE				
solvent	supporting electrolyte	$Fe^{I}P^{-}/Fe^{I}P$	$Fe^{I}P/Fe^{II}P$	$Fe^{II}P/Fe^{III}P$	$Fe^{III}P/Fe^{III}P^{+}$	$Fe^{III}P^{+}/Fe^{IV}P^{+}$ or $Fe^{III}P^{2+}$
DMF	Et_4NClO_4	−1.64	−1.23	−0.11	+0.63	+0.86
	$LiClO_4$	−1.50	−1.05	−0.05	+0.81	+1.11
	LiCl	−1.65	−1.25	−0.08	*a*	*a*
	LiBr	−1.68	−1.22	−0.07	*a*	*a*
Me_2SO	Et_4NClO_4	−1.57	−1.15	+0.02	*a*	*a*
	$LiClO_4$	−1.57	−1.15	+0.02	*a*	*a*
	LiCl	−1.54	−1.10	0.00	*a*	*a*
	LiBr	−1.68	−1.24	−0.04	*a*	*a*
py	Et_4NClO_4	−1.78	−1.54	+0.32	*a*	*a*
	$LiClO_4$	*a*	−1.57	+0.34	*a*	*a*

[a] No reproducible peaks observed. [b] Cyclic voltammograms were measured at glassy carbon in oxygen-free solutions at a scan rate of 0.04 V s^{-1} and are referenced to SCE. $[ClFeTBP]/M = (0.5–1.0) \times 10^{-3}$.

complexes, we analyzed the ligand field by conventional methods.[19] The coefficients of the basis function in ground-state Kramers doublets, and subsequently the tetragonal (μ) and rhombic splitting (R), were calculated in units of the spin–orbit coupling constant (λ) from the observed g values. The results are shown in Table I, together with those for hemoprotein– and tetraphenylpoprhine–imidazole complexes. The obtained values are characteristic in that both μ and R are fairly small compared to μ and R values of normal porphyrins. Since stronger ligand field ligands give a larger tetragonal splitting in the series of low-spin complexes,[18] the small μ values found here in the presence of a strong-field ligand such as imidazole must indicate that the Cl–Fe interaction in $ClImFe^{III}TBP$ or $Cl(Im)_2Fe^{III}TBP$ is weaker than in general bis(imidazole) type porphyrins. Since $ClFe^{III}TBP$ has no peripheral substituent, the fact that both $ClImFe^{III}TBP$ and $Cl(Im)_2Fe^{III}TBP$, whose symmetries are presumed to be axial, produced three g values indicates that the R value predominantly represents the distortion of the heme skelton. In this context, the small R value implies that the distortion of the (tetrabenzoporphinato)iron skeleton is not as great as that of the general heme skeleton.

The EPR spectrum in pyridine (curve D) is peculiar, giving three signals at ca. $g = 6$, 4.3, and 2.

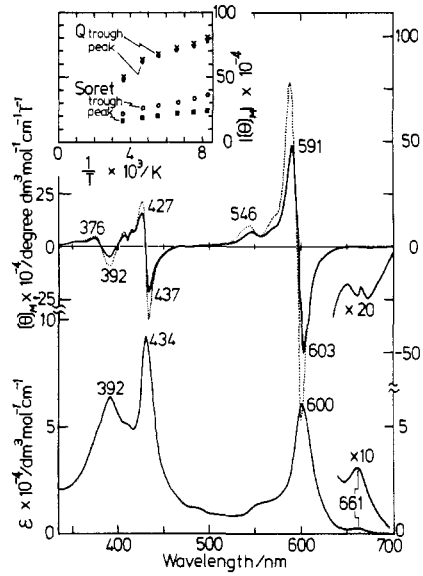

Figure 3. Absorption (bottom) and MCD (top) spectra of ClFeTBP in pyridine at ambient temperature (solid line) and at 121 K (dotted line). The inset shows the temperature dependence of MCD intensity at the Soret and Q bands ($[ClFe^{III}TBP]/M = 1.99 \times 10^{-5}$, path length 5 and 2 mm for the measurements at room temperature and at cryogenic temperature, respectively).

(ii) Cyclic Voltammetry. Figure 2 shows the cyclic voltammograms (i–E curves) for H_2TBP and $ClFe^{III}TBP$. The important experimental parameters obtained for various solvents and supporting electrolytes are summarized in Table II. FeTBP revealed typically five pairs of peaks over the potential range scanned. The redox couples close to 0 V are due to iron, and as can be judged from the EPR spectrum in Figure 1A, these couples correspond to the $Fe^{III/II}TBP$ couple. Other redox couples that can be attributed, from the change of electronic absorption and MCD spectra shown below, to $Fe^{II/I}TBP$ and $Fe^{III}TBP$ and the $Fe^{III}TBP$ cation radical appear at around −1.2 and +0.6–0.8 V, respectively. The $Fe^{III/II}TBP$ and $Fe^{II/I}TBP$ couples are solvent sensitive but insensitive to counteranions (X, electrolyte). This behavior can be explained by the greater dissociation of the Fe–X bond. The positions of $Fe^{III/II}TBP$ redox couples are between those of $Fe^{III/II}TPP$[20] and $Fe^{III/II}TDPc$ ((tetrakis(decyloxy)phthalocyaninato)iron), an iron(III) high-spin phthalocyanine.[7]

(iii) Electronic Absorption and Magnetic Circular Dichroism. Table III summarizes the main features of the electronic absorption spectra of FeTBP in various solvent systems. Compared with those of normal porphyrins,[6] Q bands are much more intense and are shifted markedly in the red direction. $ClFe^{III}TBP$ produced similar spectra[21,22] in solvents such as $CHCl_3$, CH_2Cl_2, acetone, benzene, DMF, Me_2SO, and chlorobenzene and appears to exist as iron(III) high-spin-state complex, since it gave EPR

(19) (a) Taylor, C. P. S. *Biochim. Biophys. Acta* **1977**, *491*, 137–149. (b) Griffith, J. S. *Nature (London)* **1957**, *180*, 30–31. (c) Weithbluth, M. *Struct. Bonding (Berlin)* **1967**, *2*, 1–125. (d) Griffith, J. S. "The Theory of Transition-Metal Ions"; Cambridge University Press: New York, 1967. (e) Stevens, K. W. H. *Proc. R. Soc. London, Ser. A* **1953**, *219*, 542–555.

(20) Sattelee, J. D.; LaMar, G. N.; Frye, J. S. *J. Am. Chem. Soc.* **1976**, *98*, 7275–7282.

(21) ClFeTBP may be coordinated by one or two solvent molecule(s) when dissolved in potentially coordinating solvents such as DMF, Me_2SO, and alcohols. There are two tractable means to verify displacement of halogen counteranion by solvent molecules. One is the electrochemical titration of ClFeTBP in noncoordinating solvent with potentially coordinating solvent. By the analysis of cathodic potential shifts of iron redox couple with increasing [coordinating solvent], the displacement is inferred.[22] The application of this method to the present system was found difficult because of the low solubility of ClFeTBP in noncoordinating solvents. The other is to use spectroscopic methods for the above process. This method is quite reliable if K_1 (complex formation constant between a porphyrin and a solvent molecule to form a porphyrin coordinated by a solvent molecule) and K_2 (complex formation constant between a porphyrin singly coordinated by a solvent molecule and the second solvent molecule to form a porphyrin doubly coordinated by the solvent molecule) values are markedly different from each other. This method was, however, not as valid for the present system, since K_1 and K_2 values were found to be comparable (part v).

(22) Crow, D. R. "Polarography of Metal Complexes"; Academic Press: London, 1969.

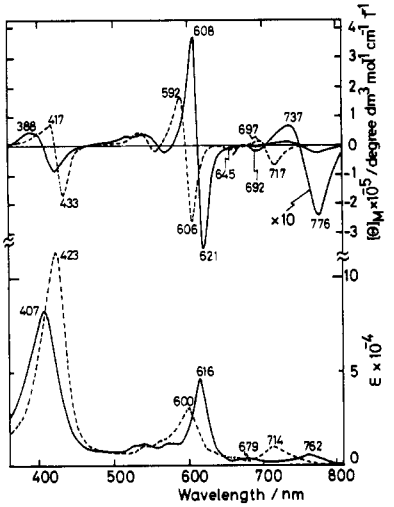

Figure 4. Electronic absorption (bottom) and MCD (top) spectra of $ClFe^{III}TBP$ in $CHCl_3$ (solid line) and in Me_2SO containing 0.1 M LiCl (broken line) ($[ClFe^{III}TBP]/M = 2.48 \times 10^{-5}$ and 4.05×10^{-5} for UV and MCD spectra in $CHCl_3$, respectively, and 1.3×10^{-5} in Me_2SO, field 1.1 T, path length 1 cm).

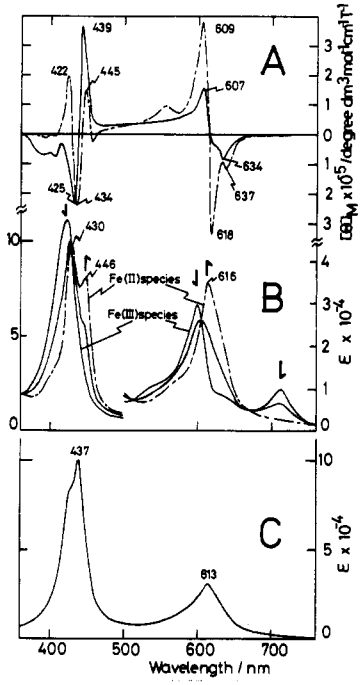

Figure 5. (A) MCD spectra of $Fe^{II}TBP$ chemically produced from $ClFe^{III}TBP$ by 15-crown-5 and $Na_2S_2O_4$ in $CHCl_3$–MeOH (4:1 v/v) (solid line) and electrochemically prepared $Fe^{II}TBP$ in Me_2SO containing 0.1 M LiCl (broken line) (magnetic field 1.1 T, path length 10 mm for the former and 1 mm for the latter). (B) Electronic absorption spectra accompanying electrochemical reduction from $ClFe^{III}TBP$ to its iron(II) species. Bold arrows indicate the direction of the spectral change. (C) Absorption spectra of iron(II) species obtained chemically by treating $ClFe^{III}TBP$ with 15-crown-5 and $Na_2S_2O_4$ in $CHCl_3$–MeOH (4:1 v/v) (path length 10 mm).

spectra with g values around 6 and 2 in $CHCl_3$ and in CH_2Cl_2. The positions of the near-infrared bands (charge-transfer transition from porphyrin $a_{1u}(\pi)$ and $a_{2u}(\pi)$ to iron $e_g(d\pi)$ orbitals) in these solvents are situated at shorter wavelengths than those of general iron(III) porphyrins (>800 nm)[23] in accord with the prediction from molecular orbital calculation.[24] On the other hand, the

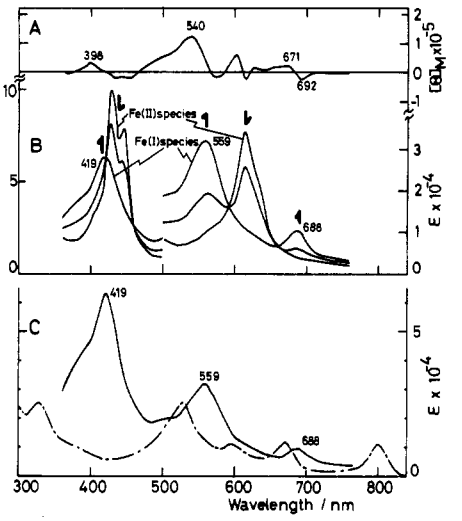

Figure 6. (A) MCD spectra of FeTBP obtained by electrochemical reduction of $Fe^{II}TBP$ in Me_2SO containing 0.1 M LiCl. (path length 1 mm, $[FeTBP]/M = 1.40 \times 10^{-4}$). (B) Change in absorption spectra corresponding to (A). (C) Absorption spectra of $Fe^{I}TBP$, replotted from (B) (solid line), and $Fe^{I}Pc$ as reference, replotted from ref 26b (broken line).

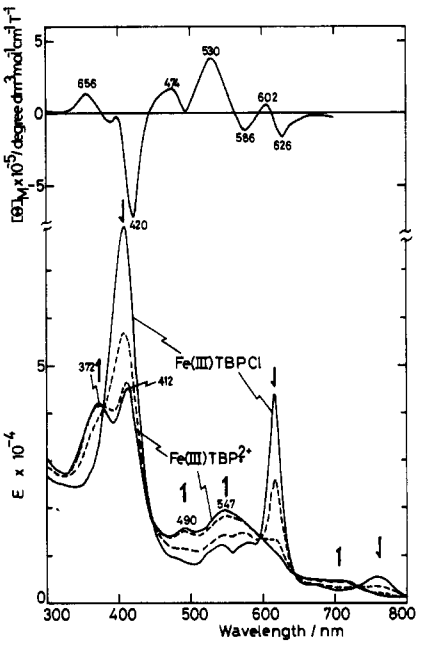

Figure 7. MCD (top) and absorption (bottom) spectra of chemically oxidized one-electron-oxidation product of $ClFe^{III}TBP$ in CH_2Cl_2 ($[FeTBP]/M = 1.4 \times 10^{-5}$, [phenoxathiin hexachloroantimonate]/M = 1.5×10^{-5}, field 1.1 T). Bold arrrows indicate the direction of spectral change.

spectrum in pyridine (Figure 3) is quite different from the others and practically the same as that reported in ref 2b in pyridine–methanol (1:10 v/v). Although they assigned the species in this mixed solvent to be the low-spin iron(II) bis(pyridine) complex on the basis of the lack of an EPR signal at temperatures between 45 and 77 K, the following observations lead us to a different assignment: (i) the EPR spectrum in Figure 1 (curve D) suggests the coexistence of Fe(III) high- and intermediate-spin species; (ii) temperature dependence of MCD intensity is not appropriate for Fe(III) low-spin[25] or for Fe(II) high- or low-spin[26] species;

(23) Kobayashi, N.; Nozawa, T.; Hatano, M. *Biochim. Biophys. Acta* **1977**, *493*, 340–351. (b) Nozawa, T.; Yamamoto, T.; Hatano, M. *Ibid.* **1976**, *427*, 28–37. (c) Kobayashi, H.; Kaizu, Y.; Tsuji, K. 45th Annual Meeting of the Chemical Society of Japan, Tokyo, April 1982, Abstract No. 2B36. (d) Smith, D. W.; Williams, R. J. P. *Struct. Bonding (Berlin)* **1970**, *7*, 1–45.

(24) Lee, L. K.; Sabelli, N. H.; LeBreton, P. R. *J. Phys. Chem.* **1982**, *86*, 3926–3931.

(25) (a) Kobayashi, H.; Higuchi, T.; Eguchi, K. *Bull. Chem. Soc. Jpn.* **1976**, *49*, 457–463. (b) Vickery, L.; Nozawa, T.; Sauer, K. *J. Am. Chem. Soc.* **1976**, *98*, 343–350, 351–357. (c) Hatano, M.; Nozawa, T. *Adv. Biophys.* **1978**, *11*, 95–149.

Table III. Absorption Maxima and Extinction Coefficients for ClFeTBP in Various Solvents[a]

solvent	λ_{max}/nm ($\epsilon \times 10^{-3}$)	solubility[b]
chloroform	762 (4.5), 616 (45.9), 578 (11.6), 543 (11.3), 407 (80.3)	2.9×10^{-4}
dichloromethane	762 (5.0), 616 (46), 578 (11.6), 543 (11.3), 407 (81.1)	1.3×10^{-4}
benzene	757 (5.6), 670 (3.4), 616 (43.8), 581 (18), 544 (12.7), 412 (76.7)	2.1×10^{-4}
chlorobenzene	760 (6.2), 670 (4.1), 618 (48.5), 580 (13.3), 545 (13.3), 412 (78.6)	2.4×10^{-4}
tetrahydrofuran	723 (6.5), 605 (31.6), 575 sh (14.8), 540 (10.9), 418 (106)	4.7×10^{-4}
acetone	754 (5), 614 (43), 580 (14), 540 (12.5), 405 (89)	1.8×10^{-4}
methanol	677 (15.8), 581 (13.8), 510 (15.6), 415 (101)	ca. 8×10^{-5}
N,*N*-dimethylformamide	716 (8.4), 602 (74.4), 536 (10.2), 418 (95.2)	1.4×10^{-3}
dimethyl sulfoxide	714 (9.6), 600 (30.1), 540 (10.4), 407 (112.3)	1.1×10^{-3}
pyridine	661 (3.0), 600 (60.2), 434 (92.0), 392 (64.4)	5.6×10^{-3}

[a] As shown in part iv, since the spectra change by the concentration of the porphyrin, data were obtained at [ClFe^{III}TBP]/M = (3 ± 1) × 10^{-5} except those in DMF (ca. 10^{-4}). Typically, for example, a peak at 677 nm in CH_3OH splits into two peaks at 603 and 730 nm with the increase of [ClFe^{III}TBP]. [b] Of a saturated solution at 22 ± 1 °C. In moles per liter.

(iii) spectral titration in DMF suggests that in pyridine the system is composed mainly of a mono(pyridine) adduct with little amount of a bis(pyridine) adduct.

Figures 4–7 show absorption and MCD spectra of chemically or electrochemically reduced FeTBP and chemically oxidized FeTBP. At every reduction and oxidation step, several isosbestic points were observed. As will be described below, two characteristics distinctively different from those of normal porphyrins are the MCD intensity in the Q-band region being generally larger than in the Soret region and the Soret optical band often splitting into two peaks.

Solid curves in Figure 4 are for ClFe^{III}TBP in $CHCl_3$. As expected from the EPR spectrum in Figure 1, spectra are typical[27] for Fe(III) high-spin porphyrins: a positive *A* term (a change in sign from minus to plus on the lower energy side) and a negative trough appeared associated with 762- and 679-nm absorption peaks, respectively. From the similarity in shape in the near-infrared region, ClFe^{III}TBP seems to be in a high-spin state in Me_2SO.

Figure 5 represents the spectra of the first reduction product. Although it is difficult to judge the oxidation and spin states from the spectra of electrochemically reduced species, the Soret MCD spectrum of a chemically reduced species (sign change from plus to minus on the lower energy side) suggests[25] that this species is an Fe(II) high-spin-state complex. Moreover, since four-coordinate square-planar iron(II) porphyrins are known to have two bands of roughly equal intensity of opposite signs in the Soret region,[28] this species may not have any axial ligand.

Figure 6 displays the spectra of the second reduction product. This species appears to be Fe^{I}TBP because of the following criteria,[29] though the possibility of Fe^{II}TBP anion cannot be ruled out completely: (i) The spectral change accompanying reduction of Fe^{II}TBP is that which has been observed for reduction of Fe(II) porphyrin to Fe(I) porphyrin; i.e., the intensity of the Soret band decreased markedly and shifted to the blue, and in the visible region, peaks appeared at both the shorter and the longer wavelength side of the peak of Fe(II) porphyrin. (ii) As for other Fe(I) porphyrins,[29a] the spectra of reduced species depend significantly on the nature of the solvent, but only slightly on the electrolyte. (iii) Though the spectrum is situated fairly far in the blue, its pattern, especially that of the MCD, resembles that of Fe(I) phthalocyanine[7b,29b,30] (see also Figure 6c).

Figure 7 shows the spectra after a one-electron oxidation[12,31] with phenoxathiin hexachloroantimonate. Though the absorption spectrum in the Soret region splits into two peaks, it appears to be that of the π cation radical of ClFe^{III}TBP, since Fe(III) porphyrin π cation radicals generally produce a very broad Soret band and a simple visible band monotonously decreasing toward the lower energy side.[31] MCD yielded positive *A* terms corresponding to every absorption peak and shoulder.

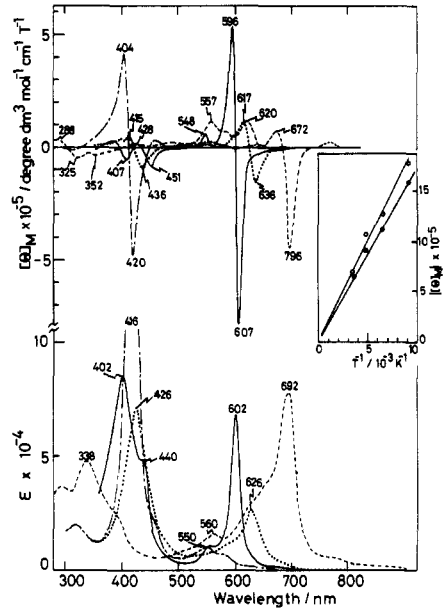

Figure 8. MCD (top) and electronic absorption (bottom) spectra of ClIm$_2$Fe^{III}TBP in DMF (solid line), ClImFe^{III}TBP in $CHCl_3$ (dotted line), ClIm$_2$FeTPP in $CHCl_3$ (dotted broken line), and ImFe^{III}TDPc in CH_2Cl_2 (broken line). The spectrum of ImFe^{III}TDPc was replotted from ref 7a. For the mono(imidazole) derivative, initial [ClFe^{III}TBP]/M = 2.48×10^{-5} and [Im]/M = 5×10^{-2}, and for the bis(imidazole) derivative, initial [ClFe^{III}TBP]/M = 2.03×10^{-5} and [Im]/M = 5 Initial [ClFeTPP]/M = 7.78×10^{-6}, and added [Im]/M = 2×10^{-2}. The inset shows the temperature dependence of the MCD intensity of the visible peak and trough of ClIm$_2$Fe^{III}TBP in DMF (path length 2 mm, temperature 283, 213, 153, and 110 K, magnetic field 1.45 T).

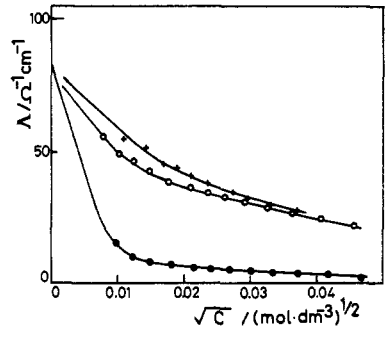

Figure 9. Molar conductance of ClFe^{III}TBP (○), ClFe^{III}TPP (●), and BrFe^{III}TPP (+) as a function of concentration in DMF.

(26) (a) Stephens, P. J. *J. Chem. Phys.* **1970**, *52*, 3489–3516. (b) Stephens, P. J.; Suetaka, M.; Schatz, P. N. *Ibid.* **1966**, *44*, 4592–4602. (c) Sutherland, J. C.; Klein, M. P. *Ibid.* **1972**, *57*, 76–86.
(27) Yamamoto, T.; Nozawa, T.; Kobayashi, N.; Hatano, M. *Bull. Chem. Soc. Jpn.* **1982**, *55*, 3059–3063 and some references therein.
(28) Collman, J. P.; Brauman, J. I.; Doxee, K. M.; Halbert, T. R.; Bunnenberg, E.; Rinder, R. E.; Gaudio, J. D.; Lang, G.; Spartalian, K. *J. Am. Chem. Soc.* **1980**, *102*, 4182–4192.
(29) Lex, D.; Momenteau, M.; Mispelter, J. *Biochem. Biophys. Acta* **1974**, *338*, 151–163. (b) Lever, A. B. P.; Wilshire, J. P. *Inorg. Chem.* **1978**, *17*, 1145–1150.
(30) Clack, D. W.; Yandle, J. R. *Inorg. Chem.* **1972**, *11*, 1738–1742.
(31) Carnieri, N.; Harriman, A. *Inorg. Chim. Acta* **1982**, *62*, 103–107.

Table IV. Approximate Conditions Required to Obtain Mono- and/or Dibase Adducts of $ClFe^{III}TBP$ in Some Solvents

solvent	initial $[ClFe^{III}TBP]/10^{-5}$ M ①	base	[base]/M required to form monobase adduct ②	②/①	[base]/M required to form dibase adduct ③	③/①
$CHCl_3$	2.03	Im	2×10^{-3}–5×10^{-2}	100–2500	*a*	
		2-MeIm	$(6–7) \times 10^{-3}$	ca. 300–350	*a*	
	1.15	*N*-MeIm	10^{-2}–10^{-1}	1000–10000	>ca. 2.5	>ca. 220000
CH_2Cl_2	2.03	Im	1.8×10^{-3}–4×10^{-2}	90–2000	*a*	
		2-MeIm	$(5–6) \times 10^{-3}$	ca. 250–300	*a*	
	1.15	*N*-MeIm	10^{-2}–10^{-1}	1000–10000	>ca. 2.5	>ca. 220000
DMF	2.03	Im	*b*		>ca. 1	>ca. 50000
	1.15	*N*-MeIm	*b*		>ca. 5	>ca. 500000

[a] Even though [base] was increased to the saturation, relatively pure dibase adduct could not be obtained. [b] Relatively pure monobase adduct could not be recognized, because of the presence of several equilibria.

Table V. Comparison of the Absorption Spectra among FeTPP, FeTBP, FeTDPc, and FePc and Some of Their Derivatives[a]

compd	wavelength of main abs peak/nm ($\epsilon \times 10^{-3}$) soret	vis	near-IR	solvent (electrolyte)	remarks spin state	others	ref
$ClFe^{III}TPP$	417 (99.1)	510 (12.6)	876 (0.5)	$CHCl_3$	high		29
$ClFe^{III}TBP$	407 (80.3)	616 (45.9)	762 (4.5)	$CHCl_3$	high		
$Fe^{III}TDPc$	337 (50.5)	652 (53.3)	825 (13.2)	CH_2Cl_2	high		7c
$Fe^{II}TPP$	431 (123)	563 (8.8)		DMF	high		26a
$Fe^{II}TBP$	430 (98.0) 446 (80.5)	616 (35.0)		Me_2SO (0.1 M LiCl)		*b*	
	437 (100)	613 (30.4)		$CHCl_3$–MeOH (4:1 (v/v))	high	*c*	
$Fe^{II}TDPc$	320 (40.5) 363 (40.2)	667 (78.4)		Me_2SO (0.2 M Bu_4NCl)	low	*b*	7c
$Fe^{II}Pc$	323 (16.3)	653 (81.3)		Me_2SO	low		32b
$Fe^{I}TPP$	390 (35.7) 420 (36.9)	510 (12) 580 (8.7)		Me_2SO (0.1 M LiCl)		*b*	26a
$Fe^{I}TBP$	419 (63.2)	559 (31.7) 688 (10.3)		Me_2SO (0.1 M LiCl)		*b*	
$Fe^{I}TDPc$	332 (40.2)	550 (38.0) 654 (29.7)	820 (13.3)	Me_2SO (0.2 M Bu_4NCl)	low	*b*	7c
$Fe^{I}Pc$	327 (25.0)	515 (25.0) 661 (24.6)	801 (11.8)	Me_2SO (0.1 M LiCl)	low	*b*	26b
$(SbF_6)ImFe^{III}TPP$	413 (*d*)	511 (*d*)		toluene	high		34
$ClImFe^{III}TBP$	426 (70.8)	626 (26.8)		$CHCl_3$	low		
$ImFe^{III}TDPc$	339 (48.4)	692 (65.9)	1085 (0.17) 1195 (0.19)	CH_2Cl_2	low		7c
$Cl(Im)_2Fe^{III}TPP$	417 (154)	549 (9.04)	1164 (0.211) 1458 (0.198)	$CHCl_3$	low		29
$Cl(Im)_2Fe^{III}TBP$	402 (84.0) 440 (46.9)	602 (67.2)		DMF	low		
$(Im)_2Fe^{II}TDPc$	350 (57.0) 440 (20.0)	672 (83.9)		CH_2Cl_2	low		7c

[a] Axial ligands of reduced species are not included. [b] Electrochemical reduction. [c] Reduction with 18-crown-6 and $Na_2S_2O_4$. [d] Data not available.

Figure 8 shows the spectra of imidazole adducts of $ClFe^{III}TBP$. The species in DMF and $CHCl_3$–MeOH (1:1 v/v) mixture were identified to be $Cl(Im)_2Fe^{III}TBP$ and $ClImFe^{III}TBP$,[21] respectively, from the change in optical spectra when imidazole was added to the solution containing $ClFe^{III}TBP$ (see, for details, part v). As with usual Fe(III) low-spin porphyrins,[25] the MCD intensity at the Soret and main Q bands increased linearly with the reciprocal of absolute temperature (inset). Extrapolation to infinitely high temperatures leads to a *y* intercept of $[\theta]_M = 0$, indicating a contribution from only a Faraday *C* term. Consistent with the results from EPR (Figure 1), the Q-band MCD of $ClImFe^{III}TBP$ was also found to be composed of only a *C* term.

(iv) Interaction between Iron and Halide Counteranion in $ClFe^{III}TBP$. In order to characterize $ClFe^{III}TBP$ further, we examined the Fe–Cl interaction by spectroscopy and by measurement of the conductance of various $ClFe^{III}TBP$ solutions (DMF).[21] Displayed in Figure 9 are molar conductance (Λ) vs. $[ClFe^{III}TBP]^{1/2}$ plots, together with those of $ClFe^{III}TPP$ and $BrFe^{III}TPP$. At all concentrations examined, the conductivity of $ClFe^{III}TBP$ is much larger than that of $ClFe^{III}TPP$ and is nearly the same magnitude as that of $BrFe^{III}TPP$. Though not shown, $1/\Lambda$ vs. $[ClFe^{III}TBP]$ plots gave a linear relationship in the concentration range studied, indicating that $ClFe^{III}TBP$ is actually a weak electrolyte. Along with the fact that the interactions between $Fe^{III}TPP$ and halide counteranions decrease markedly on going from $ClFe^{III}TPP$ to $BrFe^{III}TPP$,[32] the above data reveal that the Fe–Cl interaction in $ClFe^{III}TBP$ is weaker than that in $ClFe^{III}TPP$.

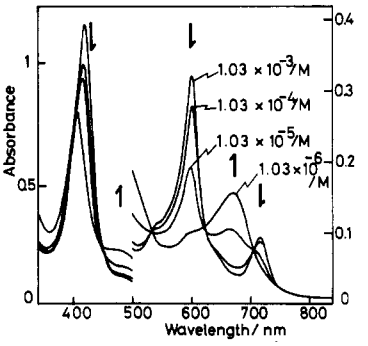

Figure 10. Spectral changes as a function of $[ClFe^{III}TBP]$ in DMF.

Figure 10 depicts the spectral changes observed as a function of $[ClFe^{III}TBP]$ in DMF. The data are displayed such that the product of concentration of $ClFe^{III}TBP$ times the optical pathlength is a constant at all concentrations of $ClFe^{III}TBP$. With the decrease of $[ClFe^{III}TBP]$, the Q band moves to the lower energy side, while the Soret band shifts to the higher energy side.

(32) Walker, F. A.; Lo, M. W.; Ree, M. T. *J. Am. Chem. Soc.* **1976**, *98*, 5552–5560.

As shown in Figure 9, this transformation in the chromophore is associated with the change in ionic strength and therefore with the extent of dissociation of Cl^- counteranion. The halide is completely dissociated at $[ClFe^{III}TBP]/M$ = ca. 10^{-6}. The phenomenon here may thus be expressed by either one or both of the equations

$$ClFeTBP \rightleftharpoons FeTBP^+ + Cl^- \quad (1)$$

$$ClFeTBP(DMF)_n \rightleftharpoons FeTBP(DMF)_n^+ + Cl^- \quad n = 1, 2 \quad (2)$$

This figure also indicates that the near-IR charge-transfer (CT) band (in this case at 716 nm) characteristic of Fe(III) high-spin porphyrins fades away with the increased dissociation of the counteranion.[33,34]

(v) Ligation of Strong Bases to $ClFe^{III}TBP$ in Various Solvents. In the reactions of iron(III) high-spin porphyrins or iron(II) phthalocyanines with strong bases to form their mono- and subsequently dibase adducts, it is known that the complex formation constant in the former process (K_1's) are much smaller than those in the latter process (K_2's). However, we reported recently[7] that a complete inverse relationship (K_1's >> K_2's) exists in the reaction between iron(III) high-spin phthalocyanines and strong bases. From this, it was expected that the ratio of K_1/K_2 would increase in the sequence $ClFe^{III}TPP$ < $ClFe^{III}TBP$ < Fe^{III} high-spin phthalocyanine. Hence, trials to obtain accurate sets of complex formation constants were attempted by various methods[35] but ended unsuccessfully probably because of the ease of dissociation of halide counteranion. By addition of strong bases to the solution containing $ClFe^{III}TBP$, the increase in dissociation of the halide was always recognized spectroscopically. Isosbestic points were not recorded except in a few cases. Nonetheless, by examining many previous reports[36] and comparing present data with theirs, we could obtain conditions necessary for the formation of relatively pure monobase and/or dibase adducts in some solvents (Table IV). If we compare the conditions used to obtain K_1 and K_2 values between $ClFe^{III}TPP$[35a] or Fe^{III} high-spin phthalocyanine[7] and strong bases with those in Table IV, it is apparent that the K_1/K_2 value increases in the sequence anticipated above. The mono- and dibase adducts of $ClFe^{III}TBP$ are, as shown in the above sections, iron(III) low-spin complexes except for the pyridine adduct.

(vi) Solubility. A quantitative determination of the solubilities of $ClFe^{III}TBP$ in various solvents is presented in Table III. As pointed out already in the comparison among some phthalocyanines and tetrabenzoporphyrins,[37] $ClFe^{III}TBP$ is substantially more soluble than iron phthalocyanine without any substituent groups. Although the absorption spectra in nonpolar solvents such as benzene do not differ markedly by $[ClFe^{III}TBP]$, those in polar solvents change significantly depending on the concentration. So, care must be taken in determining $[ClFe^{III}TBP]$ in polar solvents from the UV data in Table III. Typically, for example, a peak at 677 nm in methanol splits into two peaks at 603 and 730 nm when the porphyrin concentration is increased.

Concluding Remarks

The present study concludes that $ClFe^{III}TBP$ actually is in several aspects an intermediary compound between iron(III) high-spin porphyrins (such as $ClFe^{III}TPP$) and iron(III) high-spin phthalocyanines (such as $Fe^{III}TDPc$): (i) Fe–halide counteranion interaction decreases in the order of $ClFe^{III}TPP$, $ClFe^{III}TBP$, and perhaps $Fe^{III}TDPc$. (ii) The magnitude of the ratio in complex formation constants with bases, i.e. K_1/K_2, increases in the above order. (iii) Iron(III/II) redox potential shifts anodically in the above sequence. (iv) As represented typically by the spectra of iron(III) complexes (Table V), the position and intensity of absorption bands of $ClFe^{III}TBP$ and its derivatives situate roughly between those of ClFeTPP and FeTDPc. (v) Ligand field strength increases in the order tetraphenylporphinato dianion < tetrabenzoporphinato dianion < 4,4′,4″,4‴-tetrakis(decyloxy)-phthalocyaninato dianion. This statement is based on the following observations: (a) $ClFe^{III}TPP$ and $(SbF_6)ImFe^{III}TPP$[38] contain high-spin Fe^{III}, while $Cl(Im)_2Fe^{III}TPP$ contains low-spin Fe^{III}. (b) $ClFe^{III}TBP$ contains high-spin Fe^{III}, while $ClImFe^{III}TBP$ and $Cl(Im)_2Fe^{III}TBP$ contain low-spin Fe^{III}. (c) $Fe^{III}TDPc$ contains high-spin Fe^{III}, while $ImFe^{III}TDPc$ and $(Im)_2Fe^{II}TDPc$ are Fe^{III} and Fe^{II} low-spin complexes, respectively.[7]

Acknowledgment. We thank Dr. M. Kozuka for his courtesy in measuring EPR spectra and Prof. Y. Nishiyama for his encouragement. This work was partially supported by a Grant-in-Aid for Scientific Research from the Ministry of Education, No. 59750698.

Registry No. ClFeTBP, 85245-61-0; ClImFeTBP, 96667-05-9; $Cl(Im)_2$FeTBP, 96667-06-0; $[FeTBP]^{2-}$, 96667-07-1; $[FeTBP]^-$, 96667-08-2; [FeTBP], 22878-89-3; $[FeTBP]^+$, 96667-09-3; $[FeTBP]^{2+}$, 96667-10-6; Cl(2-MeIm)FeTBP, 96667-14-0; Cl(*N*-MeIm)$_2$FeTBP, 96667-15-1; Cl(*N*-MeIm)FeTBP, 96667-11-7; Cl(py)FeTBP, 96667-12-8; $Cl(py)_2$FeTBP, 96667-13-9.

(33) We confirmed this fact separately using $ClFe^{III}TPP$ and $BrFe^{III}TPP$. Accordingly, it may be sometimes dangerous to judge that the porphyrin is not in the iron(III) high-spin state by the lack of this CT band. If the intensity of this band in the iron(III) high-spin-state porphyrin is weak, it may inversely be possible to conclude that dissociation of halide counteranion is large.[34]

(34) Kobayashi, N.; Shirai, H.; Hojo, N. *J. Chem. Soc., Dalton Trans* **1984**, 2107–2110.

(35) (a) Rossoti, F. J. C.; Rossoti, H. "The Determination of Stability Constants"; McGraw-Hill: New York, 1961, pp 270–327. (b) Ang, K. P. *J. Chem. Phys.* **1958**, *62*, 1109–1112.

(36) (a) Pasternack, R. F.; Gillies, B. G.; Stahlbush, J. R. *J. Am. Chem. Soc.* **1978**, *100*, 2613–2619 and references 10, 14, 19, 22–24, and 42–44 cited therein. (b) Jones, J. G.; Twigg, M. V. *Inorg. Chim. Acta* **1975**, *12*, L15 and references cited therein; **1974**, *10*, 103–108.

(37) Barret, P. A.; Linstead, R. P.; Rundal, F. G.; Tuey, G. A. P. *J. Chem. Soc.* **1940**, 1079–1093.

(38) Quinn, R.; Nappa, M.; Valentine, J. S. *J. Am. Chem. Soc.* **1982**, *104*, 2588–2595.